URSI AP-RASC 2019, New Delhi, India; 09 - 15 March 2019

Phenomenological Modeling of Millimeter-Wave Automotive Radar

Zora Slavik*(1) and Kumar Vijay Mishra(2)
(1) FZI Forschungszentrum Informatik, Karlsruhe, Germany
(2) The University of Iowa, Iowa City, IA 52242 USA

Abstract

Automotive radars are an increasingly essential element in advanced driving assistance systems (ADAS) in order to make autonomous driving feasible. The automotive market segment is highly sensitive to price. This imposes additional constraints on the development of robust and reliable vehicular sensors. In order to ensure a high quality in testing and yet minimize the time-to-market, virtual and semi-virtual testing have gained more currency lately. It allows safe testing while including adverse conditions and enables low-cost evaluation of new experimental radar architectures. In this paper, we introduce and validate a phenomenological radar sensor simulation at millimeter wave that allows for virtual performance analysis of an automotive radar system in realistic environmental conditions. In particular, we extract effects from adverse weather conditions from field measurements and translate their characteristics to stimuli-generating models. Finally, we directly evaluate our radar simulation via state-of-the-art noise-waveform-based automotive radar with real interference signals.

1 Introduction

Advanced driving assistance systems (ADAS) are on a rise to enable automated transportation systems, reduce fatal traffic accidents, improve traffic flows and increase sustainability [1]. Autonomous ADAS functionalities go far beyond passenger comfort features, while the system complexity is increasing. Hence, the testing procedure of these functions exceeds manageable efforts. Therefore, (semi-)virtual validation and verification are required to preserve an acceptable overall system safety and reliability [2]. For example, recent initiatives such as European Initiative to Enable Validation for Highly Automated Safe and Secure Systems (ENABLE-S3) [3] propose to enable virtual testing for automated systems with reasonable efforts and time [4]. The joint simulation platform of ENABLE-S3 features a complete harvesting simulation wherein the system under test (SUT) is equipped with virtual automotive controls and sensors including the radar sensor simulation and adverse weather stimulation.

Often radar sensor simulations are implemented at target or object list level that comprises of targets' measured distance, azimuth, Doppler velocity and reflectivity [5, 6]. This approach approximates visual perception without electro-magnetic characteristics or features from the radio-frequency (RF) front-end. However, it is simpler and less computationally demanding than, for instance ray-tracing models [7, 8] that offer high simulation accuracy. In between these two approaches, phenomenological radar modeling fills the gap in the sense that it is accurate wherever necessary and simplifies models wherever sufficient.

In this paper, we develop a phenomenological radar model that mimics the physical characteristics of real sensors such as individual antenna elements and arrays and validate it with a set of test measurements. Our goal is to determine the impact of adverse weather conditions and spectral interference on sensors as well as evaluate concepts for millimeter-wave automotive radars [9, 10]. Our simulations reflect near-field effects of unfavorable environmental conditions such as splash water on the radar and transfer the results to data-driven models for stimulation generation. In addition, we implement a pulsed-Doppler noise radar using the validated radar sensor model and compare its performance with the legacy frequency-modulated continuous-wave (FMCW) system in the specific context of spectral interference. Our results indicate convergence of simulated and real data and robust interference performance of the pulsed automotive radar systems.

2 FZI Automotive Radar Sensor Model

Typical automotive radars track a maximum range of up to 200 m traffic moving at minimum relative velocities from 10 to 80 km/h. Most of the commercial automotive radars transmit linear FMCW chirps because of its simple electronics and low-cost. Compared to the signal at high intermediate-frequencies (IF) in pulsed-Doppler radars, the digital acquisition in FMCW radar samples the low-frequency beat signal obtained from mixing the transmit and receive signals. The frequency difference between the two signals is caused by the propagation path to a reflecting object and a Doppler shift induced by moving radar platforms or objects. In case of dense traffic with multiple FMCW radars operating simultaneously, each system may experience interference unless their basebands are separated in time or frequency domains. However, both time and spectral resources are finite and alternative techniques [1] are required to mitigate vehicle-to-vehicle (V2V) interference. In particular, the pulsed waveform approach that employs noise waveforms [10] acts as an individual fingerprint of each transmitter and, thereby, makes it robust

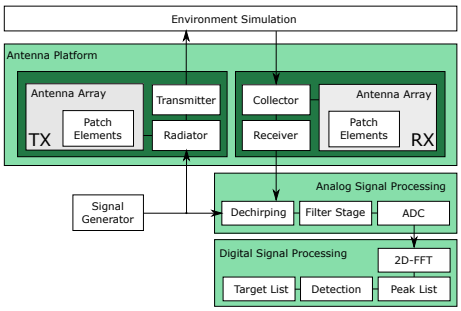

Figure 1. Block diagram of FZI radar sensor simulation including signal processing and environment model. Each block represents interchangeable modules. Both transmit (TX) and receive (RX) antenna arrays and RF chains reflect physical characteristics of the original radar system. Other components are an arbitrary signal generator and virtual analog and digital processing blocks.

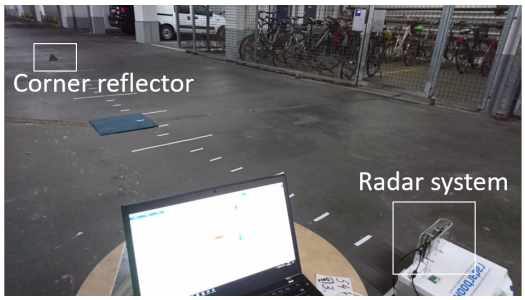

Figure 2. Experiment setup for validation measurements. A real radar is employed to record reflected echoes from a corner reflector. The FZI sensor model simulates the radar behavior in a virtual environment.

against V2V interference.

Simulation requirements and interfaces are still not standardized in automotive testing including radar, which limits the re-usability of simulators [11] and therefore requires not only the permanent development of sensor models tailored to particular applications, but also to individually interpret and translate outputs from different environment simulations. The modularity of the radar sensor model developed at Forschungszentrum Informatik (FZI), Karlsruhe allows a low-key adaptation of transmit waveforms, signal acquisition, processing and interfacing with different environment simulations. Thus leads to a flexible evaluation platform (Figure 1) that simulates backscatter signals according to multiple, physical radar sensor characteristics.

The FMCW beat signal is accessible in both, real and virtual radar systems, we recorded the beat signal for validating the sensor model as per the experimental setup shown in Figure 2. Our validation process involves simulation of a corner reflector as a point scatterer. The surrounding structures such as the columns and walls in a parking garage were neglected as can be seen from a comparison of the simulated and measured range-azimuth map in Figure 3, but which is part of ongoing further work.

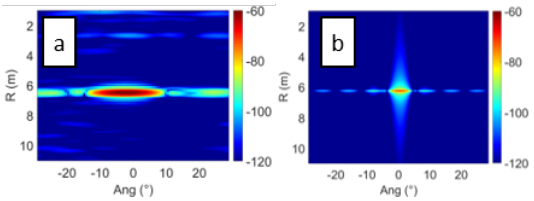

Figure 3. Raw time-series data plotted as a map of range ('R') and azimuth ('Ang') bins for the (a) real and (b) simulated radar data.

Table 1. ITU-R visibility codes and 77 GHz attenuation

Precipitation	Intensity [mm/h]	Visibility [m]	γ_R @ 77 GHz [dB/10m]
Storm	100	770	0.3081
Strong rain	25	1900	0.1140
Average rain	12.5	2800	0.0693
Light rain	2.5	5900	0.0218
Drizzle	0.25	18100	0.0042

The radar sensor simulator (Figure 4) shows the directivity of a single patch element used in both, transmit and receive antenna arrays.The transmit antenna employs four uniform linear arrays (ULAs), spaced at $7\lambda/2$, with eight patch elements each. These are switched on sequentially and, therefore, have lower gain and diminished directivity than the simultaneously operating eight receive ULAs with inter-element spacing $\lambda/2$.

3 Sensor Modeling of Weather Conditions

Apart from the target characteristics, our sensor model also allows for reproducing effect of rain. Table 1 lists the visibility by various precipitation rates and specific attenuation (or range derivation of attenuation) according to [12] specifications. Here, visibility refers to the distance at which the contrast drops by 2 % at wavelength 550 nm. The specific attenuation γ_R at 77 GHz corresponds to the far-field propagation [13, 14] and depends on the rain rate R as $\gamma_R = kR^\alpha$ according to the ITU recommendation [15], where the experimentally determined coefficients k, α are given for different frequencies.

At the ranges that are typical for automotive scenarios and that rarely exceed 200 m, the specific rain attenuation has only insignificant impact (see Table 1). However, adverse weather conditions introduce effects in the ultimate vicinity of the sensor. Just as the camera lenses are blurred from falling rain drops [16], a radome covered by water also experiences a blur and signal attenuation [17]. To extract meaningful and relevant features for realistic radar signal stimulation, we mounted the reference radar at a fixed range from several static reflecting objects at the same elevation as the radar such as depicted in Figure 5. This highly controlled environment was designed to isolate effects that are solely due to weather conditions. Several dynamic scenarios were experimented with, for example, splash water, dry radome and repetitive application of water sprinkles Figure 6. The radome material may exhibit its own intrinsic

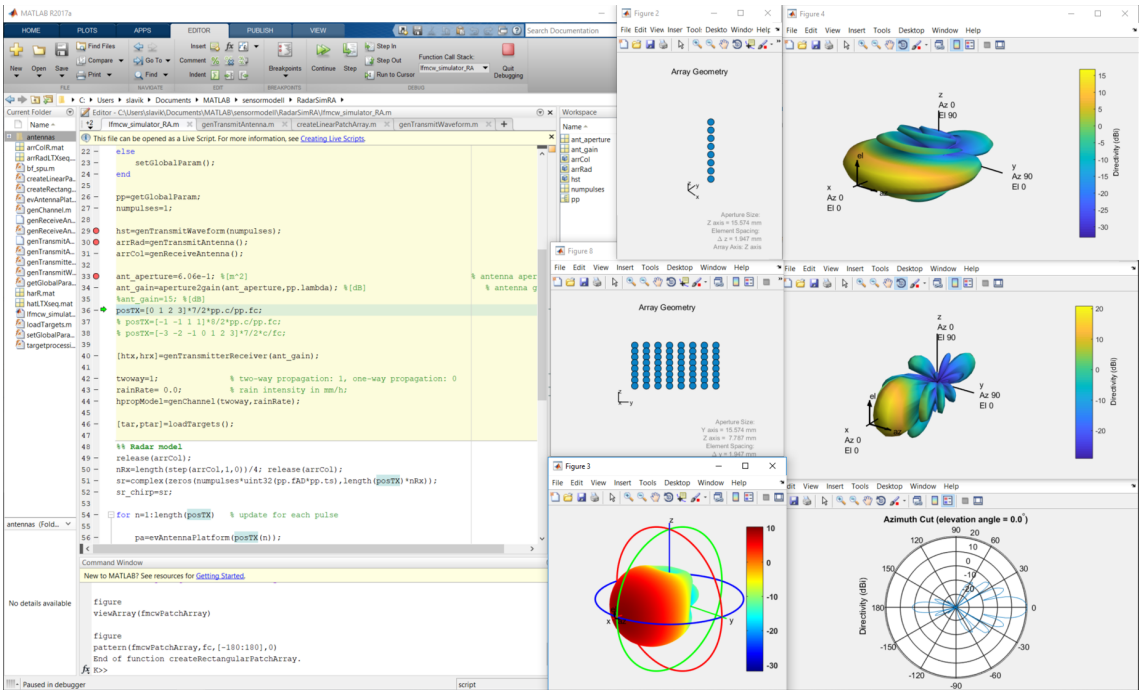

Figure 4. Radar sensor simulator display. Transmit and receive antenna arrays and directivity.

Figure 5. Experiment setup to measure effects of adverse weather conditions. Two targets are mounted in front the radar that is mounted in a box with additional sensors such as a camera. The radar radome was exposed to different water applications representing drizzle or splash water.

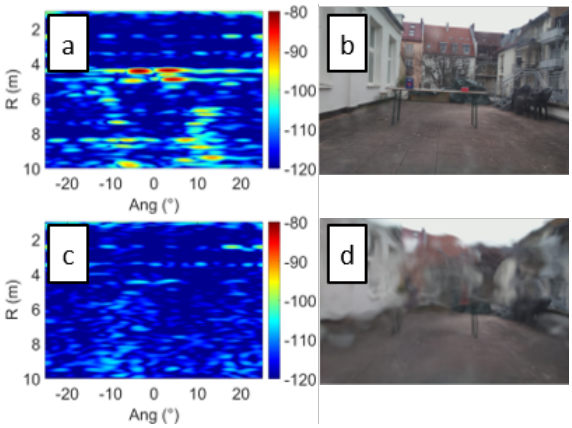

Figure 6. Resulting range-azimuth maps from measurements taken during the experiment in Figure 5: (a) initially dry radome and (b) the corresponding camera view, (c) radome during splash water application and (d) the corresponding camera view.

time-varying or constant attenuation. However, regarding the example for aggregation of peak attenuation over time during splash water in Figure 7, the type of adverse weather and environment conditions can be understood. These experimental measurements establish the base for data-driven adverse weather models. In order to model the radome attenuation, our simulator accounts for the specific rain attenuation, attenuation from constant water coverage, splash water and other attenuation from dynamic water coverage. Splash water attenuation such as in Figure 7 is modeled as $a_{sw}(t) = \sum_{p=0}^{P-1} \alpha_p \cdot a_{sw}(t - \tau_p)$, where P is the number of splash water incidents, $a_{sw}(t)$ is attenuation due to splash water, and α_p is a scaling factor that refers to the fraction of the radome surface hit by a splash after time span τ_p.

4 Performance Evaluation for Interference

We also analyzed the performance of FMCW and a noise-modulated pulsed-Doppler radar using the FZI phenomenological radar sensor model. The FMCW radar receiver is unable to distinguish if the spectral components within the beat signal result from reflecting objects or interference. Hence, additional spikes occur in the range profile obtained after dechirping and 2-D FFT processing (top panel in Figure 8). On the other hand, the correlation-based receiver of the proposed noise radar eliminates the interference (bottom panel in Figure 8) because the latter is orthogonal to the coded noise.

5 Acknowledgements

This work has been conducted within the ENABLE-S3 project funded by the ECSEL Joint Undertaking (JU) under grant agreement no 692455, supported by the Euro-

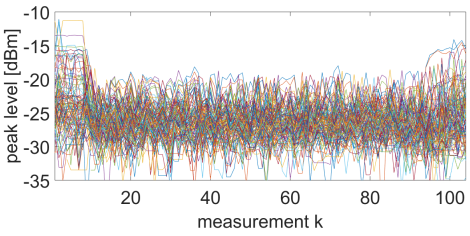

Figure 7. Aggregation of peak attenuation during the application of splash water. The plot represents several detected peaks in range direction.

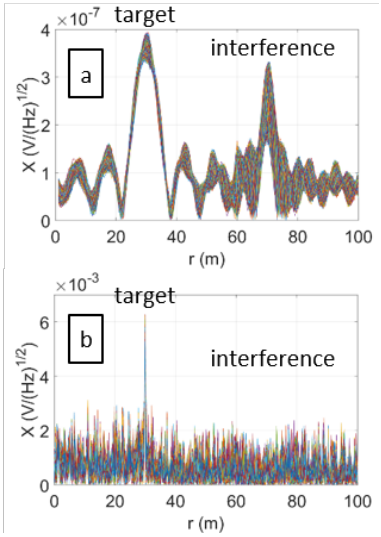

Figure 8. Impact of interference in (a) FMCW and (b) noise radar system.

pean Union's HORIZON 2020 research and innovation program. Additionally, this work was partially supported under the Federal Ministry of Education and Research (BMBF) grant 16ESE0132. Z.S. acknowledges partial support by the State of Baden-Wuerttemberg, Germany, Ministry of Science, Research and Arts within the cooperative graduate program EAES of the University of Tuebingen. K.V.M. acknowledges support from Iowa Flood Center.

References

[1] K. V. Mishra, A. Zhitnikov, and Y. C. Eldar, "Spectrum sharing solution for automotive radar," in *IEEE Vehicular Technology Conference - Spring*, 2017, pp. 1–5.

[2] C. Sturm, S. Knorzer, T. Zwick, and W. Wiesbeck, "Virtual performance evaluation of automotive radar concepts in realistic traffic environments," in *International Conference on Electromagnetics in Advanced Applications*, 2009, pp. 206–209.

[3] European Initiative to Enable Validation for Highly Automated Safe and Secure Systems. [Online]. Available: https://www.enable-s3.eu

[4] M. Rooker, P. Horstrand, A. S. Rodriguez, S. Lopez, R. Sarmiento, J. Lopez, R. A. Lattarulo, J. M. P. Rastelli, J. Matute, Z. Slavik, D. Pereira, M. Pusenius, and T. Leppälampi, "Towards improved validation of autonomous systems for smart farming," in *Workshop on Smart Farming at CPS Week*, Porto, Portugal, 2018.

[5] S. Bernsteiner, Z. Magosi, D. Lindvai-Soos, and A. Eichberger, "Radar sensor model for the virtual development process," *ATZelektronik worldwide*, no. 2, pp. 46–52, 2015.

[6] E. Roth, T. J. Dirndorfer, A. Knoll, K. von Neumann-Cosel, T. Ganslmeier, A. Kern, and M.-O. Fischer, "Analysis and validation of perception sensor models in an integrated vehicle and environment simulation," in *Enhanced Safety of Vehicles Conference*, 2011.

[7] G. Herz, B. Schick, R. Hettel, and H. Meinel, "Sophisticated sensor model framework providing real sophisticated sensor model framework providing realistic radar sensor behavior in virtual environments," in *Graz Symposium Virtual Vehicle*, 2017.

[8] N. Hirsenkorn, P. Subkowski, T. Hanke, A. Schaermann, A. Rauch, R. Rasshofer, and E. Biebl, "A ray launching approach for modeling an FMCW radar system," in *International Radar Symposium*, 2017, pp. 1–10.

[9] K. V. Mishra and Y. C. Eldar, "Sub-Nyquist channel estimation over IEEE 802.11ad link," in *IEEE International Conference on Sampling Theory and Applications*, 2017, pp. 355–359.

[10] Z. Slavik, A. Viehl, T. Greiner, O. Bringmann, and W. Rosenstiel, "Compressive sensing-based noise radar for automotive applications," in *IEEE International Symposium on Electronics and Telecommunications*, 2016, pp. 17–20.

[11] M. F. Holder, V. P. Makkapati, P. Rosenberger, T. D'hondt, Z. Slavik, F. M. Maier, H. Schreiber, Z. Magosi, H. Winner, O. Bringmann, and W. Rosenstiel, "Measurements revealing challenges in radar sensor modeling for virtual validation of autonomous driving," in *IEEE International Conference on Intelligent Transportation Systems*, 2018, in press.

[12] *Propagation data required for the design of terrestrial free-space optical links*, Recommendation ITU-R P.1817-1 ed., Geneve, 2012.

[13] M. Thurai, K. V. Mishra, V. Bringi, and W. F. Krajewski, "Initial results of a new composite-weighted algorithm for dual-polarized X-band rainfall estimation," *Journal of Hydrometeorology*, vol. 18, no. 4, pp. 1081–1100, 2017.

[14] K. V. Mishra, V. Chandrasekar, C. Nguyen, and M. Vega, "The signal processor system for the NASA dual-frequency dual-polarized Doppler radar," in *IEEE International Geoscience and Remote Sensing Symposium*, 2012, pp. 4774–4777.

[15] *Specific attenuation model for rain for use in prediction methods*, Recommendation ITU-R P.838-3 ed., Geneve, 2005.

[16] D. Hospach, S. Mueller, J. Gerlach, O. Bringmann, and W. Rosenstiel, "Simulation and evaluation of the influence of sensor characteristics on vision based Advanced Driver Assistance Systems," in *IEEE International Conference on Intelligent Transportation Systems*, 2014.

[17] K. V. Mishra, W. F. Krajewski, R. Goska, D. Ceynar, B.-C. Seo, A. Kruger, J. J. Niemeier, M. B. Galvez, M. Thurai, V. Bringi *et al.*, "Deployment and performance analyses of high-resolution Iowa XPOL radar system during the NASA IFloodS campaign," *Journal of Hydrometeorology*, vol. 17, no. 2, pp. 455–479, 2016.